Atmos. Chem. Phys. Discuss., 11, 25327–25369, 2011
www.atmos-chem-phys-discuss.net/11/25327/2011/
doi:10.5194/acpd-11-25327-2011


Atmospheric Chemistry and Physics Discussions



# Assessing filtering of mountaintop $CO_2$ mixing ratios for application to inverse models of biosphere-atmosphere carbon exchange

**B.-G. J. Brooks[1], A. R. Desai[1], B. B. Stephens[2], D. R. Bowling[3], S. P. Burns[2], A. S. Watt[2], S. L. Heck[2,4], and C. Sweeney[5]**

[1]Center for Climatic Research, University of Wisconsin-Madison, Madison, WI, USA
[2]National Center for Atmospheric Research, Boulder, CO, USA
[3]Department of Biology, University of Utah, Salt Lake City, UT, USA
[4]Department of Atmospheric and Oceanic Sciences, University of Colorado, Boulder, CO, USA
[5]Earth System Research Laboratory, NOAA, Boulder, CO, USA

Received: 30 June 2011 – Accepted: 26 August 2011 – Published: 12 September 2011

Correspondence to: B. Brooks (bjorn@climatemodeling.org)

Published by Copernicus Publications on behalf of the European Geosciences Union.







## Abstract

There is a widely recognized need to improve our understanding of biosphere-atmosphere carbon exchanges in areas of complex terrain including the United States Mountain West. $CO_2$ fluxes over mountainous terrain are difficult to measure often due to unusual and complicated influences associated with atmospheric transport in complex terrain. Using five years of $CO_2$ mixing ratio observations from the Regional Atmospheric Continuous $CO_2$ Network in the Rocky Mountains (Rocky RACCOON), five statistical (subsetting) filters are used to investigate a range of approaches for identifying regionally representative $CO_2$ mixing ratios. Test results from three filters indicate that subsets based on short-term variance and local $CO_2$ gradients across tower inlet heights retain nine-tenths of the total observations and are able to define representative diurnal variability and seasonal cycles even for difficult-to-model sites where the influence of local fluxes is much larger than regional mixing ratio variations. Test results from two other filters that consider measurements from previous and following days using spline fitting or sliding windows are overly selective. Case study examples showed that even when standardized to common subset sizes these windowing-filters rejected measurements representing synoptic changes in $CO_2$, which suggests that they are not well suited to filtering continental $CO_2$ measurements. We present a novel $CO_2$ lapse rate filter that uses $CO_2$ differences between levels in the model atmosphere to constrain subsets of site measurements that are representative on model scales.

## 1 Introduction

The Western United States is suspected to have substantial carbon sinks with uptake that is strongly determined by ecosystem dynamics in complex terrain above 750 m (Schimel et al., 2002; Hu et al., 2010). Carbon cycle inverse models that assimilate $CO_2$ mixing ratios to infer land-atmosphere $CO_2$ fluxes present an excellent opportunity for identifying the magnitude and climate sensitivity of these different carbon





ACPD
11, 25327–25369, 2011



sinks in the Mountain West (Raupach, 2011). There are however two major issues when using carbon cycle inversion models in complex terrain. First, carbon-cycle inversion model topographies are often too coarsely gridded to represent complex terrain resulting in large mismatches (e.g., $10^3$ m) between the actual surface elevation and the model surface elevation. Second, winds used to drive inversion models are not always accurate, particularly in complex terrain, and may incorrectly inform the model about the source region of assimilated measurements.

Detailed research has greatly improved understandings about the causes of $CO_2$ variability over several well studied mountainous sites (e.g., Pérez-Landa et al., 2007; Sun et al., 2010), however the airflow patterns at such sites cannot be assumed to be representative of all variability across the US Mountain West. $CO_2$ mixing ratios must be precisely measured by a network of sites throughout the region and filtered to remove observations that are strongly influenced by local sources and sinks. Although filtering (i.e., subsetting) reduces the number of observations available for use as assimilation constraints, filtering is necessary in order to distinguish the model-resolvable biotic changes in regional $CO_2$ fluxes caused for example by photosynthesis, respiration, and disturbance (Boisvenue and Running, 2010; Medvigy et al., 2010) from larger diurnal and seasonal variations that are driven by complex terrain transport (Stewart et al., 2002; Yi et al., 2008).

Until recently much of the Mountain West region between Colorado and Nevada (Fig. 1) represented a large gap in the monitoring coverage of continuous $CO_2$ mixing ratio measurements, which has limited our ability to determine its relative importance as a carbon sink. The Mountain West region spans a large portion of the Western US, where ecoregions are abruptly divided by physiographic barriers that give rise to complex $CO_2$ source and sink regions associated with heterogeneous plant distributions and climate drivers. Although site-scale eddy flux towers such as the Niwot Ridge AmeriFlux tower can capture local (e.g., 1 $km^2$) net ecosystem exchange (NEE, Monson et al., 2002; Hu et al., 2010) these measurements may not be representative of regional changes (e.g., 10 000 $km^2$).





ACPD
11, 25327–25369, 2011



Regional scale boundary layer budgets are difficult to construct (Desai et al., 2011), which leaves atmospheric tracer-transport inversion modeling as one of few ways to constrain regional carbon budgets. An important limitation however, has been that global inverse carbon cycle models based on coarse resolution atmospheric models use highly smoothed topography and thus do not adequately represent the observing height relative to ground or topographic influences at the observing sites. Consequently, these models have trouble representing transport of $CO_2$ by local circulations (at scales below 10 000 $km^2$, cf. Gerbig et al., 2003) and terrain induced advective flows (Sun et al., 2007; Yi et al., 2008; Burns et al., 2011). There is a need to identify well-mixed regional air mass measurements corresponding to the resolution of one model grid cell over smoothed terrain for accurate retrievals of $CO_2$ fluxes by tracer-transport inversion (Denning et al., 2002; Gurney et al., 2002; Gerbig et al., 2003; Lin et al., 2004; de Wekker et al., 2009).

Mountaintop observations of $CO_2$ mixing ratios are of great interest because stations at high elevation can frequently be subject to descending well-mixed air masses that may be suitable for assimilation by inverse models. Our goal in this study is to partition from the complete set of mountaintop $CO_2$ mixing ratios those observations that are representative of air on spatial scales corresponding to the transport model resolution of state-of-the-art carbon cycle inversion models. We use measurements from the Regional Atmospheric Continuous $CO_2$ Network in the Rocky Mountains (raccoon.ucar.edu). Datasets from the still-growing RACCOON network range back though August, 2005. However, as described earlier, the complete set of these data contain samples representing both local and regional air influences that necessitate filtering. Analyses of these filtered subsets permits us to: (1) determine if hourly-statistical filters of $CO_2$ time series, which do not consider past and future $CO_2$ variability, are sufficient for identifying local or regional air masses as a way to "flag" data prior to assimilation into an inverse model; and (2) investigate how these filters compare to $CO_2$ filters that utilize preceding and following $CO_2$ mixing ratios and variability to determine cutoff ranges.





ACPD
11, 25327–25369, 2011



## 2 Background

### 2.1 Importance of regionally representative $CO_2$ mixing ratios

Inverse modeling with atmospheric tracer-transport has been used to derive biosphere-atmosphere carbon dioxide exchanges (Göckede et al., 2010; Peters et al., 2010; Gurney and Eckels, 2011). However, since most coarse-resolution atmospheric transport models used in inversions are not able to simulate variations in $CO_2$ at scales below 10 000 km$^2$ (e.g., Peters et al., 2010) it is necessary to filter $CO_2$ measurements representing small scale influences prior to assimilation.

When estimating carbon cycle flux parameters and magnitudes by inverse techniques (e.g., Bayesian synthesis inversion, geostatistical inverse modeling, ensemble Kalman filtering) unfiltered data that include measurements representative of small-scale local influences (especially in complex terrain, e.g., Turnipseed et al., 2004) can lead to model parameters that do no accurately represent the process of interest. Regional representativeness of the data can be improved by selectively partitioning measurements that are likely to be representative of well mixed air masses on scales of 10 000 km$^2$. Filtering data, however, poses challenges. The spatial and temporal scale coverage of automated regional observation networks makes flagging measurements "by hand" impossible and requires robust autonomous filtering approaches. Given that co-located meteorological data are not always available, our goal was to use statistical filters that operate on the $CO_2$ mixing ratios alone.

Until recently, most carbon-cycle inversion models avoided much of the need for filtering observations because they assimilated monthly or annually averaged $CO_2$ often sampled from remote marine boundary layer sites (Tans et al., 1990; Enting and Mansbridge, 1991; Fan et al., 1998). This has changed with the present class of inversion models (e.g., Göckede et al., 2010; Peters et al., 2010; Schuh et al., 2010), which assimilate $CO_2$ mixing ratios and compute fluxes on sub-daily scales using high frequency observations taken from many locations including continental sites. In dealing with spatial representativeness issues of high frequency observations ensemble





ACPD
11, 25327–25369, 2011



assimilation strategies, including variance inflation (Hamill et al., 2001; Zupanski et al., 2007), are used to mitigate some but not all of the model error. No matter the correction strategy, removing certain observations that do not match model resolved processes is necessary to ensure that posterior fluxes optimized based on measured $CO_2$ mixing ratios are physically realistic.

Variability in the observations due to local influences not resolvable by inverse models can be several ppm to tens of ppm. In meeting our goal of partitioning $CO_2$ mixing ratios to meet the resolution of the model requires that we diagnose the performance of filters at rejecting observations representative of local-scale flux heterogeneities and unresolved topographic airflows prior to assimilation by a carbon cycle inverse model. CarbonTracker (Peters et al., 2007, 2010) is one example of an inverse data assimilation system that incorporates $CO_2$ mixing ratios including observations from Rocky RACCOON and will be referred to as an example $CO_2$ inversion system.

### 2.2 Causes of variability in $CO_2$ mixing ratios in complex terrain

The causes of $CO_2$ variability beyond the diurnal and seasonal cycles of carbon dioxide measured at Rocky Mountain locations (see Fig. 2) have been a topic of study for several decades (Gillette and Steele, 1983). Deviations from the signal of well-mixed free-tropospheric carbon dioxide can be difficult to model for several reasons. Although upwind sources and sinks of $CO_2$ commonly have a primary influence on mixing ratios recorded at the measurement site, in complex terrain this is often found not to be the case during the morning transition when prevailing winds slacken and upslope flows become more influential (Bowling et al., 2011). Strong upslope flows or weak winds can result in prominent $CO_2$ spikes in time series, often on the order of several ppm and lasting a few hours or less. This is not the case for all terrain flows however, as some actually provide favorable mountaintop sampling conditions characterized by $CO_2$ signals that do not deviate substantially. Filters or combinations of filters provide robust automated methods for rejecting measurements with limited spatial representativeness.





ACPD
11, 25327–25369, 2011



In complex terrain a measurement of atmospheric $CO_2$ can be representative over large spatial scales, or it may be locally representative as can be the case during morning transitions when mountain slope warming and gentle upslope winds can be more influential than prevailing winds and turbulent mixing (Stewart et al., 2002; de Wekker et al., 2009). These air masses can sometimes be identified by their high $CO_2$ variability. Although several studies within the RACCOON domain have been able to identify the principal atmospheric transport mechanism causing variability at particular sites (Turnipseed et al., 2004; Sun et al., 2010), consistently robust methods capable of identifying problematic airflows across the entire RACCOON domain are not easily made autonomous. Therefore it is necessary to test and use filters that reject observations with small spatial representativeness (relative to the spatial resolution of the data assimilation system used to evaluate the data) based on statistical identifiers in the time series of $CO_2$. Our objective in applying filters directly to time series of $CO_2$ observations is to remove observations that do not communicate useful information to an inversion model about the regional carbon cycle without resorting to other information about terrain flows.

### 2.3 Filters of mountaintop $CO_2$ mixing ratios

Previous methods for filtering mountaintop observations of $CO_2$ have operated on either statistical bases for rejecting paired flask observations (i.e., detection error, Keeling et al., 1976), fixed rejection criteria about an interpolated curve (Gillette and Steele, 1983), or combined low pass-interpolation schemes for rejecting outliers (i.e., statistical interpolation, Thoning et al., 1989). Keeling et al. (1976) recognized that in order to improve the synoptic scale representativeness of measurements made on Mauna Loa (Hawaii) it would be necessary to remove observations from the complete $CO_2$ time series that appeared to be the consequence of local anthropogenic emissions, volcanic outgassing, and vegetation from the lower slopes of the mountain and around the island. Thoning et al. (1989) controlled for these observations by interpolating through the data points and rejecting outliers as well as using low-pass spectral filtering.





ACPD
11, 25327–25369, 2011



The statistical interpolation filter used by Thoning et al. (1989) was developed to filter measurements for a remote marine mountaintop location with influences very different from most continental sites. This filter was used to subset measurements made atop a volcano where pulses of $CO_2$ with small-scale representativeness were relatively infrequent and most measurements reflected large-scale well mixed marine air masses. Statistical interpolation (an example of which appears in Sect. 3.5) relies on rejection limits that are determined a priori and are specific to remote marine mountaintop locations. On the other hand these kinds of sliding window filters may have an advantage in constraining seasonal or diurnal variability because they take into consideration the previous and following $CO_2$ variability when filtering the data. We use a similar statistical interpolation filter in this study to examine their performance with continental data.

Another filtering approach used by current carbon-cycle inversion systems that assimilate observations on sub-daily time steps in areas of complex terrain (e.g., Peters et al., 2010) is time-of-day filtering. Time-of-day filtering assimilates only nocturnal observations during hours when the station is most likely to sample downward descending air from the free troposphere (ca. 00:00–04:00 LT). Although 00:00–04:00 LT filtering does not distinguish observations in any way aside from the measurement time it can be used in combination with other filters. Because such time-of-day filters are frequently used for inversions instead of or in combination with statistical filtering our results in several places present both the full subsets (all hours) and the subset when further constrained by time-of-day (00:00–04:00 LT).

### 2.4 Site descriptions, instrumentation, and sampling protocol

The Autonomous, Inexpensive, Robust $CO_2$ Analyzer (AIRCOA Stephens et al., 2006, 2011) is the atmospheric carbon dioxide sampling system developed for use at each RACCOON site. At the heart of the AIRCOA system is a single-cell infrared gas analyzer (IRGA). To compensate for moderate short-term noise and instrument drift, AIRCOA employ signal averaging and frequent calibrations using multiple reference gases tied to the World Meteorological Organization $CO_2$ scale.





ACPD
11, 25327–25369, 2011



Each AIRCOA system samples $CO_2$ across multiple inlet heights, which provides vertical $CO_2$ profiles across the height of the station. The complete description of these methods can be found in Stephens et al. (2006, 2011), see also: raccoon.ucar.edu.

Rocky RACCOON is an ongoing campaign to record atmospheric $CO_2$ across a topographically complex landscape using a network of six sites in Colorado, Arizona and Utah (Fig. 1). The NWR RACCOON site is located above tree-line on Niwot Ridge which is 5 km to the west and 470 m higher than the AmeriFlux forest site. Storm Peak Lab (SPL), Hidden Peak (HDP) and Roof Butte (RBA) are mountaintop facilities. Entrada Field Station (EFS) is located in a desert canyon, and observations here were stopped after 2 years because of inadequate mixing within the canyon.

The Fraser Experimental Forest site (FEF) is situated within a high elevation valley and subalpine coniferous forest about 100 km west of Denver, Colorado. Of the six RACCOON sites FEF has the strongest diurnal $CO_2$ cycle where summertime respiration can elevate nighttime $CO_2$ to 460 ppm within the valley. Due to strong diurnal variability at FEF (see Fig. 2) and local influences at EFS, RACCOON network results and statistics presented here are based on the other four sites. Specific diagnostic tests of filters were conducted with FEF data separately, as will be discussed later.

## 3 Methods

Here we describe five site-independent filtering methods chosen to represent a range of filters that are presently used to filter $CO_2$ mixing ratio data. All filters operate on hourly RACCOON $CO_2$ mixing ratio means derived from 2.5 min measurements, each with a 1 $\sigma$ precision of 0.1 ppm. Methods 1, 2 and 3 represent filters that consider the statistics of the hourly observation being evaluated. Methods 4 and 5 represent methods that filter based on the observed variability over preceding and following hours. As discussed in Sect. 2.3 results for each of the five filters will be compared with and without time-of-day (00:00–04:00 LT) filtering.





ACPD
11, 25327–25369, 2011



### 3.1 Method 1: short-term variance filtering

The short-term variance filter (SV) is a simple routine for flagging measurements with excessive hourly $CO_2$ variance under the assumption that regionally-representative conditions can be characterized by low $CO_2$ variance. The only condition set for observations belonging to SV subsets is that they must have hourly standard deviations less than 1 ppm. The 1 ppm hourly standard deviation limit is determined subjectively by considering monthly distributions of hourly variance and excluding obvious locally influenced data.

### 3.2 Method 2: short-term variance local gradient filtering using two inlets

Similar to the SV filter, the Short-term Variance Local Gradient filter (SVLG) adds one additional constraint that rejects observations at each time step with vertical $CO_2$ gradients (across the upper two inlets) larger than 0.5 ppm. Constraining for observations that represent small vertical gradients attempts to reject bias caused for example by strong local sources of poorly mixed air.

The formation of each SVLG subset of measurements is formally described in terms of time series signals. The related discrete time signal $x(t)$ is extracted from the original signal $X(t)$ where the hourly mean standard deviation at the top inlet height $\sigma_{x_h}$ is less than 1 ppm and the absolute difference in $CO_2$ mixing ratios between the top two inlet heights $|X_h(t) - X_{h-1}(t)|$ is less than 0.5 ppm. Like the 1 ppm hourly standard deviation limit, the 0.5 ppm limit is determined subjectively. CarbonTracker uses this SVLG filter in combination with time-of-day filtering to subset observations that are suitable for assimilation.

### 3.3 Method 3: short-term variance lapse rate filtering

Although filtering for excessive hourly variance and large $CO_2$ gradients has the advantage of excluding measurements that are clearly not representative of well mixed air or





ACPD
11, 25327–25369, 2011



may indicate strongly stratified air, it is not clear that the cutoff values (i.e., $\sigma < 1$ ppm, gradient $< 0.5$ ppm) are well suited for a given measurement site or inversion model resolution. Past research (Bergamaschi et al., 2006) has shown differences in near surface gradients of atmospheric tracers between transport models up to a factor of 3, which suggests a notable spread in capability between models at simulating vertical mixing. We addressed this issue using a new short-term variance lapse rate filter (SVLR) that connects the filter selectivity to the discretization (or vertical resolution) of the inversion model being used to assimilate the data. The protocol for SVLR filtering is exactly the same as SVLG except that rather than using the 0.5 ppm difference cutoff, SVLR uses a minimum and maximum $CO_2$ lapse rates (in ppm/m) that are determined from the near-surface $CO_2$ lapse rate in the model atmosphere above each measurement site over the entire model record (e.g., 2005–2009).

To develop SVLR subsets, near-surface $CO_2$ lapse rate ranges (min and max) were queried for each site's location from CarbonTracker-2009 output for afternoon (09:00–20:00 LT) and nocturnal (00:00–09:00, 21:00–23:00 LT) times of day. Filter lapse rate limits were set as the smallest and largest rates at which $CO_2$ mixing ratios lapsed with decreasing elevation. For each site minimum and maximum lapse rate limits were computed for afternoon and nocturnal times of day. These were calculated as the change in $CO_2$ between the model surface and the interface of the lowest model atmosphere level, which ranged between 42 and 52 m depending on the location and time of day. Also, we interpolated across CarbonTracker's North American-1° × 1° model domain to the spot corresponding to the locations of 3 of the RACCOON sites (NWR, RBA, SPL). Additional commentary on issues of horizontal grid coarseness of the CarbonTracker North American-1° × 1° grid and the vertical atmosphere levels appear later in the Discussion. Lapse rates for the station data were computed between the upper two inlet levels of each station which differed in height by 1 to 8 m. This differs from the ~45 m range over which the filter lapse rate limits were computed from the model data. Station lapse rates were computed for each hourly measurement as the difference in $CO_2$ between the upper two inlets divided by the difference in their heights (ppm $m^{-1}$). The





ACPD
11, 25327–25369, 2011



SVLR filter thus rejected all hourly site measurements with hourly standard deviations equal to or greater than 1 ppm and with lapse rates larger than the model-specified lapse rate limits for that time of day. All SVLR results are based on data from 3 sites (NWR, RBA, SPL) rather than 4 like other subsets. SVLR statistics do not include data from HDP because its inlets are horizontally separated rather than vertically separated, and vertical lapse rates cannot be computed.

### 3.4 Method 4: filtering of outliers using a weighted median smoother

An effective method that has been used in many signal filtering applications is the weighted median smoother (cf. Tukey, 1974). Because our intent is not necessarily to smooth but to reject $CO_2$ mixing ratios that are not regionally representative when present in the data, we have modified Tukey's method. We use a Weighted Median Filter (WM) that rejects an observation if its residual from the daily median is in excess of the summed and weighted inter-day variance for the previous two weeks.

The WM filter slides a backward-looking window over the time sequence $X(n)$ to create the related subset $x(n)$. A range of acceptable mixing ratios centered about the daily median value $\widetilde{X}(n)$ is computed dynamically at each step (day) $n$. The limits of the range are a function of the sum of differences between each sequential daily median value $[\widetilde{X}(n) - \widetilde{X}(n-1)]$ over the previous fifteen days weighted using a geometrical decay function to favor more recent variability. Thus the difference between today and yesterday is weighted at $1/2$, and the residual between yesterday and the day before yesterday is weighted $1/4$, and so on. The upper or lower limit, $l$, is computed using the difference equation:

$$l = \sum_{i=1}^{N} \frac{\widetilde{X}(n) - \widetilde{X}(n-1)}{2^n} \quad (1)$$

for which $N$ is the order of the geometric series that extends backward in time from $n$.





ACPD
11, 25327–25369, 2011



Therefore, subset $x(n)$ is composed of those elements $X_i$ from the original time series that do not exceed the limit, which is expressed as:

$$\{X_i \in x(n) : |\widetilde{X}(n) - X_i| < l\} \quad (2)$$

### 3.5 Method 5: iterative filtering of outliers from a fitted polynomial (statistical interpolation)

We also include a statistical interpolation filter (SI) that is duplicated from the method used by Thoning et al. (1989) at Mauna Loa to identify well-mixed background $CO_2$ (see the original publication for a complete explanation of the filtering protocol). SI considers past and future observations through a sliding window to reject outliers from a fitted spline. The SI filter used here has one key difference from Thoning et al. (1989), which is that it does not use a low-pass spectral filter.

Following the protocol outlined by (Thoning et al., 1989) our SI filter works by passing a ten day sliding window over the original discrete time signal $X(n)$ to create subset $x(n)$ that is centered at $n$ and consists initially of non-afternoon samples $X_i(n)$ for $i \leq 15$ samples (the 15 hourly $CO_2$ mixing ratios belonging to day $n$ and excluding hours 11, 12, ..., 19). Daytime values are initially excluded by Thoning et al. (1989) in order to fit the spline to values not strongly influenced by afternoon photosynthesis. For each window a cubic spline $S(X)$ is fitted through the daily means of $X_i(n)$. If the daily standard deviation ($\sigma_{X(n)}$) exceeds 0.5 ppm the filter will reject the hourly observation $X_i$ at $n$ with the largest residual from spline curve $S(X)$, which is described by the expression:

$$\{X_i \notin x(n) : \max|S(X_i) - (X_i + \sigma_{X_i})|\} \quad (3)$$

where the residual is computed as the absolute difference between the spline curve and the hourly measurement plus its hourly standard deviation ($X_i + \sigma_{X_i}$).

The window advances across all $n$'s, re-fitting a new ten day spline with each new window and rejecting no more than one observation per day with each iteration over





ACPD
11, 25327–25369, 2011



the entire time series. After no more than 14 iterations (the maximum number of hourly observations that can be rejected for each day), or when the standard deviation of all daily means is less than 0.5 ppm (e.g., $\sigma$ of $X_1(n)$, $X_2(n)$, ... $< 0.5$) the excluded daytime observations $X_j$ from the original time series (i.e., hours 11, 12, ..., 19) that are within 0.5 ppm of the final refitted spline curve are incorporated back in to form the final subset, which is expressed as:

$$\{X_j \in x(n) : |S(X_i) - X_j| < 0.5\} \quad (4)$$

where $S(X_j)$ represents the $CO_2$ value of the spline curve at corresponding moment $j$.

Figure 3 illustrates the impact of our various filters on one year of measurements for one RACCOON site (Storm Peak).

### 3.6 Meteorological data

To test each filter under various scenarios including synoptic scale frontal systems we selected case studies for the NWR station where both $CO_2$ and meteorological data were available. These meteorological data were obtained from the Saddle climate station located 150 m up-ridge from the NWR RACCOON site. We extracted variables (barometric pressure, dew point, wind direction, wind speed) and focused on frontal passages that showed longer-lived $CO_2$ shifts resulting from synoptic weather changes.

## 4 Results

### 4.1 Site filtering statistics

$CO_2$ inversion results are strongly affected not only by the number and density of observations, but also by the trends and seasonality of those data. We began by analyzing the general statistics of collective subsets representing measurements from 4 of our RACCOON sites (FEF was excluded because it reflects a special topographic setting





ACPD
11, 25327–25369, 2011



not intended to sample well-mixed air). Table 2 shows that each filter has a different selectivity and retains different numbers and types of observations. The Short-term Variance (SV), Short-term Variance Local Gradient (SVLG), and Short-term Variance Lapse Rate (SVLR) were the least selective, retaining respectively 94 %, 89 %, and 90 % of the complete set of observations (Note that all SVLR results are based on NWR, RBA and SPL sites, and do not include HDP because its inlets are not vertically separated). The two windowing-filters, WM and SI, retained only about half of the measurements across the 4 sites, 45 % and 43 %, respectively.

Combining time-of-day filtering for the complete set and the five filters results in a ∼70 % reduction in the number of observations available as constraints in assimilation, but the subset means increase only by 0.2 to 0.3 ppm for the complete set and the hourly-statistical filters (SV, SVLG, SVLR), and decrease by 0.1 ppm for the two windowing-filters (WM, SI).

The statistical spread (distribution) of each subset is shown by the deseasonalized variance that appears in Table 2. The deseasonalized variance shows that most filtering methods constrain subset variance to a narrower distribution about the mean, except for SI and SVLR (when all hours are used). Also time-of-day filtering generally has little effect on subset variability. The larger variance for SI (and smaller number of retained observations) suggests that this filtering method produces relatively sparse subsets of widely distributed values when applied to RACCOON data. SVLR, which is starred because it does not include data from the HDP site, retains most observations but still has a relatively large variance. We further tested to see whether this could be due to a bias in the number of observations during certain months or times of day, but found no significant difference between SVLR and the complete set. We can only infer from this that SVLR filtering results in subsets that have about twice the variability as the complete set.

Table 3 shows that the choice of filtering methods affects the $CO_2$ seasonality of subset observations, which may have implications for the strength and timing of retrieved NEE seasonality and carbon budgets. Subsets from statistical-filters (SV,





ACPD
11, 25327–25369, 2011



SVLG, SVLR) have seasonal amplitudes that differ by no more than −0.2 ppm from the complete set. Windowing-filters (WM, SI) have slightly larger differences in seasonal amplitude, on the order of −0.4 ppm from the complete set.

In Situ $CO_2$ lapse rates can be used to infer local $CO_2$ stratification/mixing, and can be an important consideration for model-observation representativeness issues. We investigated how lapse rates would differ between subsets, and summarized our results in Fig. 4. These subsets of RACCOON measurements broadly break into three groups that can be characterized as consistently well-mixed, reasonably well-mixed, and biased groups. In the well mixed group, SVLG and SI subsets are likely to include measurements representing well-mixed air. For the intermediate group, SVLR and SV subsets include slightly more observations representing local stratification, although SVLR appears more like the consistently well-mixed subsets except for its final downtick near $+4\sigma$. The 0–4 subset appears to be an intermediary between reasonably well-mixed and biased groups because of a final uptick near $+4\sigma$. For the biased group, the complete set and WM subset are the most likely to include stratified measurements and should be generally regarded as having measurements likely to incorrectly inform most carbon-cycle inversion models, particularly from high $CO_2$ values.

### 4.2 Comparisons to aircraft observations

We expanded our investigation by comparing filtered subsets from the Niwot Ridge (Colorado) RACCOON site (NWR) to $CO_2$ mixing ratio measurements from NOAA's bi-weekly airborne flights over Carr, Colorado, about 100 km northeast of NWR. From the 255 flights between years 2006 and 2009, 37 of them represented vertical $CO_2$ gradients less than ±1 ppm across the bottom 1500 m of the atmosphere. 24 of these 37 corresponded to hours when data were collected by the nearby NWR station.

First in order to standardize the comparison of differently filtered subsets of NWR measurements we relaxed the filtering criteria of the windowing-filters (WM, SI) in order to reject one-third of the 36 266 NWR measurements. This resulted in 20 common hourly $CO_2$ measurements between NWR and Carr. WM and SI filter criteria were





ACPD
11, 25327–25369, 2011



slackened by expanding the ppm range limits of their sliding windows by factors of 2.0 for WM and 1.68 for SI.

As opposed to WM and SI standardization, in order to standardize SV, SVLG, and SVLR we constrained their filter criteria (vertical $CO_2$ gradient and or hourly standard deviation) until obtaining 20 common measurements between each subset and Carr.

In this approach we assume that small vertical $CO_2$ gradients over Carr reflect strong vertical mixing and large spatial homogeneity in $CO_2$. Therefore, these 20 "well-mixed" reference points served as a baseline for computing biases for filtered subsets from NWR. We caution however that these common reference points are not evenly distributed across seasons. Note that there is a slight seasonal bias that tends to underrepresent months June through September. These months are only represented by 3 out of the 20 reference points, which is due to both missing hourly measurements from NWR RACCOON site in some cases and large vertical $CO_2$ gradients in the Carr data in other cases.

We noticed in our analysis that three subsets had similarly small biases from the Carr reference points. SVLG, SVLR and WM had errors (RMSE) that differed by no more than 0.05 ppm from each other and two data points or fewer, therefore we simplified their exposition in Fig. 5 by showing SVLR as an example of all three. Figure 5 indicates that when SVLG, SVLR, and WM subsets are standardized to a common subset size they are nearly equally likely to represent well-mixed air in this case study (i.e., small estimator bias (error) from Carr). Consequently these subsets have nearly the same error (RMSE $\approx$ 0.5 ppm) from the 20 well-mixed reference points. This is in contrast to the SI and SV subsets, which selected observations deviating more from Carr, and thus could be regarded as less representative of spatially homogeneous/well-mixed conditions for this case study.

### 4.3 Synoptic case studies

In the above case although three of the five filters (SVLG, SVLR, WM) were roughly equal in filtering observations representing well-mixed air, each contained slightly





ACPD
11, 25327–25369, 2011



different selections of observations, which might steer inversions differently. To investigate these selection preferences in detail we looked at several synoptic case studies representing cold front events at Niwot Ridge, two of which appear in Fig. 7. Synoptic changes in the origin of air can be critical to inversions, as they can have a larger impact on carbon dioxide mixing ratios than diurnal changes due to local changes in boundary layer height and fluxes, and carry important information on differences in upwind fluxes over large regions. Frontal passages were identified using associated meteorological data (Sect. 3.6) and retained $CO_2$ measurements were compared between subsets.

Cold front systems were identified by prolonged troughs in barometric pressure coupled to decreases in temperature, humidity, and abrupt wind direction shifts. Figure 6 shows two of the meteorological variables used (dew point, wind speed) to identify the winter frontal system that passed over NWR in February, 2007. A notable feature is the transient jump in $CO_2$ mixing ratios that is synchronous with a near 180° wind direction shift near 09:00 LT and 12:00 LT on 13 February. Particle back trajectories also indicated that the $CO_2$ jump reflects a switch in the origin of surface air from west to north-east accompanied by strong vertical shear (data not shown). This change in surface wind direction may include information important to a carbon-cycle inversion model, but that depends on the transport model's ability to resolve such airflows in the inversion.

As discussed in Sect. 4.2 in order to standardize sample sizes for the NWR site we constrained SV, SVLG and SVLR subsets to retain two-thirds of observations, and scaled-up WM and SI subsets to two-thirds by relaxing the cutoff ranges. For this case study, subsets from windowing-filters WM and SI did not retain any of the 9 measurements during the 9 h synoptic shift in wind direction. Subsets from hourly-statistical filters SV, SVLG, and SVLR retained 3, 3, and 2 of the 9 measurements in different combinations (Fig. 6), indicating a general similarity between subsets. Still these subsets do not exactly agree, which is a consequence of the difference in using hourly standard deviation, local gradient, or model-specified lapse rates in the filtering protocol.





ACPD
11, 25327–25369, 2011



For this case study subsets derived using hourly-statistical filters retained hourly $CO_2$ measurements made during the synoptic event. This indicates that SV, SVLG, and SVLR filters are capable of filtering without rejecting transient measurements that might be informative to the inversion model. On the other hand subsets from windowing filters (WM, SI) may not sufficiently represent abrupt regional-scale changes in $CO_2$ that are relevant to most state-of-the-art inversion model systems.

Filtering by time-of-day alone (00:00–04:00 LT) would result in 0 of the 9 synoptic shift observations being assimilated because the event occurs during daytime hours. Alternatively, combining time-of-day after filtering by statistical (SV, SVLG, SVLR) or windowing (WM, SI) would result in only one different observation, which occurs at 00:00 LT on 14 February in Fig. 6.

Figure 7 presents a second synoptic case study of standardized subset sizes from 4–8 June 2007, this time characterized by a shorter ∼4 h wind direction shift followed by a 2 day decline in barometric pressure and dew point. These synoptic changes resulted in a different scenario of diurnally oscillating but gradually increasing $CO_2$ mixing ratios. Subsets from SVLG and SVLR retained nearly identical collections of observations during the frontal passage near 12:00 LT on 4 June. Also SVLG and SVLR subsets, and to a limited extent SV, retained observations near daily minimum and maximum values. By contrast WM and SI subsets favored observations with $CO_2$ values near the daily mean/median and rejected values near daily extremes (00:00–04:00 and 12:00–16:00 LT). This suggests for inversion systems that use time-of-day filtering, statistical filters (e.g., SVLG and SVLR) may retain more observations than WM and SI subsets, which may be underrepresented in measurements during hours when daily extremes occur.

### 4.4 Fraser Experimental Forest

The majority of our focus until now has been on filtering measurements made at mountaintop locations that are intended for assimilation by carbon-cycle inversion models. However, not all measurement sites are so ideally located, but they may still offer





ACPD
11, 25327–25369, 2011



measurements useful as constraints for carbon-cycle inversion model systems. Here we shift our attention to examine the effectiveness of these filters for a complicated case using mixing ratios from Fraser Experimental Forest, which is located in an alpine valley at 2,745 m a.s.l. where summertime respiration can push nocturnal $CO_2$ mixing ratios above 460 ppm. Local influences at FEF are difficult to model, thus our goal is to determine if $CO_2$ observations useful to biosphere-atmosphere inversion models (on scales that can be modeled) can be extracted from FEF despite its topographic setting. Our intent is not to suggest that data from such sites be assimilated, but to diagnose and compare filters when presented with data from an extreme case.

Figure 8 shows that windowing-filters that rely on constrained diurnal $CO_2$ ranges (cf. WM, SI methods in Sects. 3.4 and 3.5) fail to locate realistic diurnal and seasonal cycles. When diurnal variability in $CO_2$ mixing ratios is high at FEF (June through November) windowing-filter subsets do not follow realistic seasonal cycles, and the subset range wanders dramatically from day to day. On the other hand statistical-filter subsets (SV, SVLG, SVLR) that do not depend on constrained diurnal variability, or observations from other time steps, identify more regionally consistent diurnal and seasonal cycles despite high diurnal $CO_2$ variability.

## 5 Discussion

In the previous section we showed that variously filtered subsets have distributions with different $CO_2$ stratifications (Fig. 4). When standardized to equal sample sizes and compared to cases of well-mixed air from airborne $CO_2$ profiles, SVLG, SVLR and WM filters were similarly capable of selecting for spatially homogeneous $CO_2$ mixing ratio measurements for the Niwot Ridge RACCOON site (Fig. 5). However, when we used case study analysis to scrutinize subset differences during frontal passages contrasts between standardized subsets from statistical and windowing-filters became evident (Figs. 6 and 7). For prolonged shifts (ca. 9 h) in air mass source regions statistical-filters (SV, SVLG, SVLR) were able to identify and retain $CO_2$ measurements despite abrupt 4–6 ppm $CO_2$ changes, while windowing-filters (WM, SI) retained none.





ACPD
11, 25327–25369, 2011



The case studies represented in Figs. 6 and 7 also show that subsets from SI and WM (the two filters that use preceding and following data to determine cutoff ranges) do not capture the diurnal variability that is particular to many continental sites. These filters would be of greater use for filtering $CO_2$ measurements from remote marine locations where diurnal variability is smaller (which was the intended use for SI in Thoning et al., 1989). Also in the above case studies it seems likely that subsets from statistical-filters (SV, SVLG, SVLR) are likely to be more informative to carbon-cycle inversion models during events that bring about synoptic scale changes in $CO_2$, however, it is not clear how selective a filter should be for measurements from a given site and a given inversion model. We addressed this problem in the SVLR filter which specifies the filter selectivity for each site and time of day by using the model as a benchmark for determining filter selectivity. As opposed to SVLG, SVLR uses near-surface $CO_2$ lapse rate limits that come from the model min and max lapse rates for each measurement location and time of day. As with SV and SVLG, SVLR does not favor measurements near daily mean values (cf. Fig. 7), and is still able to filter even when diurnal variability is large (cf. Fig. 8). Filtering in this way retains a majority of observations (86 % for 4 RACCOON sites). Figure 9 shows that these 86 % of network observations fall within narrow lapse rate ranges corresponding to lapse rates our example model can represent (see magenta colored region in Fig. 9). The remaining 14 % constitute the gray regions in Fig. 9 that represent RACCOON measurements with lapse rates larger than can be represented in the discretized model output and thus should be filtered.

The SVLR protocol relies on the assumption that model $CO_2$ lapse rates are valid indicators of the model's ability to resolve stratified atmospheric transport, which is a substantial difference from filters that rely on a priori criteria based on subjective knowledge for each site and time of day.

Figure 10 illustrates the application of the SVLR filter using CarbonTracker $CO_2$ lapse rates for a new case study during June 2007. The SVLR subset in the upper panel of Fig. 10 shows the variability in $CO_2$ mixing ratios during frontal passages near 12:00 LT on 13 June (abrupt NW to NE wind shift), near 15:00 LT on 15 June (W to S wind shift),





ACPD
11, 25327–25369, 2011



and another event near 18:00 LT on 19 June when the only substantial meteorological shift is a slackening of wind speed from 9 m s$^{-1}$ to less than 1 m s$^{-1}$ as well as large negative $CO_2$ lapse rates. The SVLR filter indicates that the 157 of 192 $CO_2$ measurements could be represented by the discretized model atmosphere. In the lower panel of Fig. 10 open circles within the magenta shaded area indicate observations rejected due to excessive statistical variance (> 1 ppm), while open circles outside the shaded area represent observations rejected due to lapse rates smaller than occur in CarbonTracker output. Although the inversion model may be able to assimilate and use the rejected observations, doing so would mean assimilating observations representing $CO_2$ stratifications (and presumably atmospheric transport processes) that cannot be represented by the model atmosphere.

Time-of-day filtering (i.e., 00:00–04:00 LT) as shown in Figs. 6, 7, 10, by itself may be a useful filtering method if no other reliable statistical filters can be employed. However, synoptic changes in $CO_2$ can be much larger than diurnal variability (cf. Fig. 6) and may occur outside of subset sampling hours thus excluding them from these subsets.

There are a few potential sources of error when extrapolating the results of our study that merit discussion here. The advantage of inversion model systems is that they optimize first-guess-fluxes using $CO_2$ mixing ratio observations, but this requires observations that are representative on spatial scales similar to the model's resolution. Although SVLR filtering uses model specified lapse rates to constrain measurements representing model resolvable air flows there is potential for false positives if SVLR falsely rejects an observation due to an excessive lapse rate when in fact the top inlet height is measuring well-mixed air. This kind of error could occur for example when unusually strong gradients near the surface (e.g., horizontal advection, van Gorsel et al., 2009) influence the lower inlets but not the uppermost inlet.

Another point of consideration for applications of the SVLR filter to a site should be the height across which lapse rates are calculated. Large height differences, or where the lower inlet is well within the canopy or close to the surface, are more likely to show large differences in $CO_2$ mixing ratios (and $CO_2$ lapse rates calculated across that





ACPD
11, 25327–25369, 2011



length). Therefore it may be necessary to apply some added flexibility to lapse rate cutoffs that are used to subset measurements from such a site.

When implementing the SVLR filter we might instead have used lapse rate limits that were seasonally specific or even specific to the month being filtered. We tried such implementations and found that it reduced the number of subset observations by one-third to one-half. Consequently we decided to use lapse rates that were specific only to the time of day because our intent with this filter is to represent the total range of possible lapse rate reproducible in the model, which has the largest difference between day and night.

Another caveat to consider is that we did not account for discrepancies in the lengths across which we computed our lapse rates from the model nor the sites. Site lapse rates were computed over lengths ranging from from 1 to 8 m, while model lapse rates were computed over length ranging from 42–52 m (if calculated as the difference between the surface and the first model atmosphere interface levels, as was used here) or 82–89.5 m (if using the middle of the model atmosphere levels). A robust implementation of our lapse rate filter would provide uncertainty in the lapse rate calculation that was based on the difference in lengths between the station and the model.

These lapse rates computed from model simulations are dependent on the model's vertical mixing, which can differ substantially between models (Bergamaschi et al., 2006). For example a model with pronounced stratification at night will appear to have larger lapse rate limits that will result in different SVLR limits as compared to another model with the same horizontal resolution but different vertical mixing. Furthermore, vertical mixing ratio gradients in TM5 Carbontracker's atmospheric transport model) may prove to be unreliable indicators of vertical mixing (Williams et al., 2011).

Our simulated lapse rates are taken from Carbontracker's North American-1° × 1° model domain. The coarseness of horizontal 1° × 1° orography also impacts the reliability of lapse rates computed across vertical levels in the atmosphere. Overall, the benefits of specifying model-based lapse rate limits may be outweighed when a coarsely discretized model is used to determine $CO_2$ gradients.





ACPD
11, 25327–25369, 2011



## 6 Conclusions

It is suspected that mountain ecosystems of the Western US are not only large stores of carbon but serve as carbon sinks, however, there is no consensus on the location or variability of potential sinks. Inverse models of biosphere-atmosphere carbon exchange that assimilate $CO_2$ mixing ratios are one of few ways to retrieve $CO_2$ fluxes in complex terrain. But model representation of important carbon-cycle changes and feedbacks in complex terrain is limited by an inability to accurately identify and assimilate $CO_2$ mixing ratios that are model resolvable. In some cases this may have resulted in inversions that are optimized from measurements reflecting $CO_2$ gradients that the model itself cannot represent. In other cases when time-of-day filtering is used (e.g., filtering for 00:00–04:00 LT measurements targeting descending air from the free troposphere) other times of day are not used to optimize prior flux estimates. Our goal in this study has been to evaluate filters in terms of their capabilities in selecting measurements that corresponded to the resolution of carbon-cycle inversion models.

Of the five filters of mountaintop measurements analyzed in this study each had its own selectivity, which resulted in: subsets of different sizes (Table 2), subsets representing air masses with different $CO_2$ stratifications (Fig. 4), and subsets that disagreed on which $CO_2$ measurements should be retained during synoptic-scale frontal passages (Figs. 6 and 7). Two filters employed here, lapse rate (SVLR) and local gradient (SVLG), provide two choices to address these issues and constrain the spatial representativeness of in situ mountaintop $CO_2$ mixing ratio measurements for stations with multiple inlet heights. The lapse rate filter (SVLR) does so by isolating a subset of measurements that correspond to the range of represented lapse rates from the inversion model, which can be an advantage of this method because it works with the limitations of the model. The local gradient filter (SVLG) performs similarly well and retains nearly the same number and kind of observations, but depends on subjective knowledge in order to establish vertical $CO_2$ gradient limits for filtering in situ measurements.





ACPD
11, 25327–25369, 2011



Lapse rate or local gradient filtering can be implemented for any carbon-cycle inversion model system using assimilated $CO_2$ mixing ratios measured across multiple inlet heights. These subsets of locally well mixed air (cf. Fig. 4) are more likely to infer regionally well mixed air corresponding to the transport model resolution of state-of-the-art carbon cycle inversion models (e.g., 10 000 $km^2$). Lapse rate and local gradient filtering of RACCOON data resulted in subsets with the smallest errors from vertically well-mixed airborne $CO_2$ profiles from Carr, Colorado (Fig. 5). The choice of SVLR or SVLG will depend on the inversion model system.

For sites where multi-inlet measurements are not available our results show that subsets based on hourly $CO_2$ variance criteria (i.e., SV) are helpful when diurnal variability is high (Fig. 8), and during synoptic changes in $CO_2$ (Figs. 6 and 7). However filtering by statistical variance alone requires that the variance limit be specified using subjective knowledge of the measurement site and in our case studies resulted in subsets that were not quite as representative of well-mixed air as SVLR, SVLG, and WM subsets (Fig. 5) and may include stratified conditions not resolvable by a model.

*Acknowledgements.* This work was supported by NOAA CPO, grant numbers NA09OAR4310065 and NA080AR4310533. The authors would also like to thank Kurt Chowanski (Institute of Arctic and Alpine Research, University of Colorado), Gannet Hallar and Ian McCubbin (Storm Peak Laboratory, Desert Research Institute), for their collaboration and providing meteorological data. We are also indebted to Andy Jacobson, Wouter Peters, and others from the NOAA Earth Systems Research Lab's CarbonTracker research group for collaboration in using RACCOON data and in discussing the CarbonTracker assimilation protocol. We thank Dean Cardinale and the Snowbird Ski and Summer Resort for their support at the Hidden Peak site. CarbonTracker 2009 results provided by NOAA ESRL, Boulder, Colorado, USA are from the website at http://carbontracker.noaa.gov.





ACPD
11, 25327–25369, 2011



## References


Bergamaschi, P., Meirink, J. F., Müller, J. F., and Körner, S.: Report on model inter-comparison performed within European Commission FP5 project EVERGREEN (Global satellite observation of greenhouse gas emissions), p. 53, EC-JRC-IES, Ispra, Italy, Sci. and Tech. Res. Ser., 2006. 25337, 25349

Boisvenue, C. and Running, S. W.: Simulations show decreasing carbon stocks and potential for carbon emissions in Rocky Mountain forests over the next century, Ecol. Appl., 20, 1302–1319, doi:10.1890/09-0504.1, 2010. 25329

Bowling, D. R., Miller, J. B., Rhodes, M. E., Burns, S. P., Monson, R. K., and Baer, D.: Corrigendum to "Soil, plant, and transport influences on methane in a subalpine forest under high ultraviolet irradiance" published in Biogeosciences, 6, 1311–1324, 2009, Biogeosciences, 8, 851–851, doi:10.5194/bg-8-851-2011, 2011. 25332

Burns, S. P., Sun, J., Lenschow, D. H., Oncley, S. P., Stephens, B. B., Chuixiang, Y., Anderson, D. E., Hu, J., and Monson, R. K.: Atmospheric stability effects on wind fields and scalar mixing within and just above a subalpine forest in sloping terrain, Bound.-Layer Meteorol., 138, 231–262, doi:10.1007/s10546-010-9560-6, 2011. 25330

Denning, A. S., Fung, I. Y., and Randall, D.: Latitudinal gradient of atmospheric CO2 due to seasonal exchange with land biota, Nature, 376, 240–243, doi:10.1038/376240a0, 2002. 25330

Desai, A. R., Moore, D. J., Ahue, W., Wilkes, P., de Wekker B. G. Brooks, S., Campos, T., Stephens, B. B., Monson, R. K., Burns, S. P., Quaife, T., Aulenbach, S. M., and Schimel, D. S.: Seasonal pattern of regional carbon balance in the Central Rocky Mountains from surface and airborne measurements, in press, doi:10.1029/2011JG001655, 2011. 25330

Enting, I. G. and Mansbridge, J. V.: Latitudinal distribution of sources and sinks of $CO_2$: Results of an inversion study, Tellus B, 43, 156–170, doi:10.1034/j.1600-0889.1991.00010.x, 1991. 25331

Fan, S., Gloor, M., Mahlman, J., Pacala, S., Sarmiento, J., Takahashi, T., and Tans, P. P.: A large terrestrial carbon sink in North America implied by atmospheric and oceanic carbon dioxide data and models, Science, 282, 442–446, doi:10.1126/science.282.5388.442, 1998. 25331

Gerbig, C., Lin, J. C., Wofsy, S. C., Daube, B. C., Andrews, A. E., Stephens, B. B., Bakwin, P. S., and Grainger, C. A.: Toward constraining regional-scale fluxes of $CO_2$ with atmospheric observations over a continent: 1. Observed spatial variability from airborne platforms, J.






ACPD
11, 25327–25369, 2011



Geophys. Res. Lett., 108, 4756, doi:10.1029/2002JD003018, 2003. 25330
Gillette, D. A. and Steele, A. T.: Selection of $CO_2$ concentration data from whole-air sampling at three locations between 1968 and 1974, J. Geophys. Res., 88, 1349–1359, doi:10.1029/JC088iC02p01349, 1983. 25332, 25333
Göckede, M., Michalak, A. M., Vickers, D., Turner, D. P., and Law, B. E.: Atmospheric inverse modeling to constrain regional scale $CO_2$ budgets at high spatial and temporal resolution, J. Geophys. Res., 115, D15113, doi:10.1029/2009JD012257, 2010. 25331
van Gorsel, E., Delpierre, N., Leuning, R., Black, A., Munger, J. W., Wofsy, S., Aubinet, M., Feigenwinter, C., Beringer, J., Bonal, D., Chen, B., Chen, J., Clement, R., Davis, K. J., Desai, A. R., Dragoni, D., Etzold, S., Grünwald, T., Gu, L., Heinesch, B., Hutyra, L. R., Jans, W. W. P., Kutsch, W., Law, B. E., Leclerc, M. Y., Mammarella, I., Montagnani, L., Noormets, A., Rebmann, C., and Wharton, S.: Estimating nocturnal ecosystem respiration from the vertical turbulent flux and change in storage of $CO_2$, Agric. Forest Meteorol., 149, 1919–1930, doi:10.1016/j.agrformet.2009.06.020, 2009. 25348
Gurney, K. R. and Eckels, W. J.: Regional trends in terrestrial carbon exchange and their seasonal signatures, Tellus B, 63, doi:10.1111/j.1600-0889.2011.00534.x, 2011. 25331
Gurney, K. R., Law, R. M., Denning, A. S., Rayner, P. J., Baker, D., Bousquet, P., Bruhwiler, L., Chen, Y.-H., Ciais, P., Fan, S., Fung, I. Y., Gloor, M., Heimann, M., Higuchi, K., John, J., Maki, T., Maksyutov, S., Masarie, K., Peylin, P., Prather, M., Pak, B. C., Randerson, J., Sarmiento, J., Taguchi, S., Takahashi, T., and Yuen, C.-W.: Towards robust regional estimates of $CO_2$ sources and sinks using atmospheric transport models, Nature, 415, 626–630, doi:10.1038/415626a, 2002. 25330
Hamill, T. M., Whitaker, J. S., and Snyder, C.: Distance-dependent filtering of background error covariance estimates in an ensemble Kalman filter, Mon. Weather Rev., 129, 2776–2790, doi:10.1175/1520-0493(2001)129<2776:DDFOBE>2.0.CO;2, 2001. 25332
Hu, J., Moore, D. J. P., Burns, S. P., and Monson, R. K.: Longer growing seasons lead to less carbon sequestration by a subalpine forest, Glob. Change Biol., 16, 771–783, doi:10.1111/j.1365-2486.2009.01967.x, 2010. 25328, 25329
Keeling, C. D., Bacastow, R. B., Bain-Bridge, A. E., Ekdahl Jr., C. A., Guenther, P. R., Waterman, L. S., and Chin, J. F. S.: Atmospheric carbon dioxide variations at Mauna Loa Observatory, Hawaii, Tellus, 28, 538–551, 1976. 25333
Lin, J. C., Gerbig, C., Daube, B. C., Wofsy, S. C., Andrews, A. E., Vay, S. A., and Anderson, B. E.: An empirical analysis of the spatial variability of atmospheric $CO_2$: implica-





ACPD
11, 25327–25369, 2011



tions for inverse analyses and space-borne sensors, Geophys. Res. Lett., 31, L23104, doi:10.1029/2004GL020957, 2004. 25330
Medvigy, D., Wofsy, S. C., Munger, J. W., and Moorcroft, P. R.: Responses of terrestrial ecosystems and carbon budgets to current and future environmental variability, P. Natl. Acad. Sci. USA, 107, 8275–8280, doi:10.1073/pnas.0912032107, 2010. 25329
Monson, R. K., Turnipseed, A. A., Sparks, J. P., Harley, P. C., Scott-Denton, L. E., Sparks, K., and Huxman, T. E.: Carbon sequestration in a high-elevation, subalpine forest, Glob. Change Biol., 8, 459–478, doi:10.1046/j.1365-2486.2002.00480.x, 2002. 25329
Pérez-Landa, G., Ciais, P., Gangoiti, G., Palau, J. L., Carrara, A., Gioli, B., Miglietta, F., Schumacher, M., Millán, M. M., and Sanz, M. J.: Mesoscale circulations over complex terrain in the Valencia coastal region, Spain – Part 2: Modeling $CO_2$ transport using idealized surface fluxes, Atmos. Chem. Phys., 7, 1851–1868, doi:10.5194/acp-7-1851-2007, 2007. 25329
Peters, W., Jacobson, A. R., Sweeney, C., Andrews, A. E., Conway, T. J., Masarie, K., Miller, J. B., Bruhwiler, L. M. P., Pétron, G., Hirsch, A. I., Worthy, D. E. J., van der Werf, G. R., Randerson, J. T., Wennberg, P. O., Krol, M. C., and Tans, P. P.: An atmospheric perspective on North American carbon dioxide exchange: CarbonTracker, P. Natl. Acad. Sci. USA, 104, 18925–18930, doi:10.1073/pnas.0708986104, 2007. 25332
Peters, W., Krol, M. C., van der Werf, G. R., Houweling, S., Jones, C. D., Hughes, J., Schaefer, K., Masarie, K. A., Jacobson, A. R., Miller, J. B., Cho, C. H., Ramonet, M., Schmidt, M., Ciattaglia, L., Apadula, F., Heltai, D., Meinhardt, F., di Sarra, A. G., Piacentino, S., Sferlazzo, D., Aalto, T., Hatakka, J., Ström, J., Haszpra, L., Meijer, H. A. J., van der Laan, S., Neubert, R. E. M., Jordan, A., Rodó, X., Morguí, J.-A., Vermeulen, A. T., Popa, E., Rozanski, K., Zimnoch, M., Manning, A. C., Leuenberger, M., Uglietti, C., Dolman, A. J., Ciais, P., Heimann, M., and Tans, P. P.: Seven years of recent European net terrestrial carbon dioxide exchange constrained by atmospheric observations, Glob. Change Biol., 16, 1317–1337, doi:10.1111/j.1365-2486.2009.02078.x, 2010. 25331, 25332, 25334
Raupach, M. R.: Carbon cycle: Pinning down the land carbon sink, Nature Clim. Change, 1, 148–149, doi:10.1038/nclimate1123, 2011. 25329
Schimel, D., Kittel, T. G. F., Running, S., Monson, R., Turnispeed, A., and Anderson, D.: Carbon sequestration studied in Western US mountains, EOS Trans., 83, 445–449, doi:10.1029/2002EO000314, 2002. 25328
Schuh, A. E., Denning, A. S., Corbin, K. D., Baker, I. T., Uliasz, M., Parazoo, N., Andrews, A. E., and Worthy, D. E. J.: A regional high-resolution carbon flux inversion of North America for





ACPD
11, 25327–25369, 2011



2004, Biogeosciences, 7, 1625–1644, doi:10.5194/bg-7-1625-2010, 2010. 25331
Stephens, B. B., Watt, A., and Maclean, G.: An autonomous inexpensive robust $CO_2$ analyzer (AIRCOA), in: 13th WMO/IAEA Meeting of Experts on Carbon Dioxide Concentration and Related Tracers Measurement Techniques, WMO TD, vol. 1359, 95–99, 2006. 25334, 25335
Stephens, B. B., Miles, N. L., Richardson, S. J., Watt, A. S., and Davis, K. J.: Atmospheric $CO_2$ monitoring with single-cell NDIR-based analyzers, Atmos. Meas. Tech. Discuss., 4, 4325–4355, doi:10.5194/amtd-4-4325-2011, 2011. 25334, 25335
Stewart, J. Q., Whiteman, C. D., Steenburgh, W. J., and Bian, X.: A climatological study of thermally driven wind systems of the US Intermountain West, B. Am. Meteorol. Soc., 83, 699–708, doi:10.1175/1520-0477(2002)083<0699:ACSOTD>2.3.CO;2, 2002. 25329, 25333
Sun, J., Burns, S. P., Delany, A. C., Oncley, S. P., Turnipseed, A. A., Stephens, B. B., Lenschow, D. H., LeMone, M. A., Monson, R. K., and Anderson, D. E.: $CO_2$ transport over complex terrain, Agr. Forest Meteorol., 145, 1–21, doi:10.1016/j.agrformet.2007.02.007, 2007. 25330
Sun, J., Oncley, S. P., Burns, S. P., Stephens, B. B., Lenschow, D. H., Campos, T., Monson, R. K., Schimel, D. S., Sacks, W. J., de Wekker, S. F. J., Lai, C.-T., Lamb, B., Ojima, D., Ellsworth, P. Z., Sternberg, L. S. L., Zhong, S., Clements, C., Moore, D. J. P., Anderson, D. E., Watt, A. S., Hu, J., Tschudi, M., Aulenbach, S., Allwine, E., and Coons, T.: A Multiscale and multidisciplinary investigation of ecosystem-atmosphere $CO_2$ exchange over the Rocky Mountains of Colorado, B. Am. Meteorol. Soc., 91, 209–230, doi:10.1175/2009BAMS2733.1, 2010. 25329, 25333
Tans, P. P., Fung, I. Y., and Takahashi, T.: Observational contrains on the global atmospheric $CO_2$ budget, Science, 247, 1431–1438, doi:10.1126/science.247.4949.1431, 1990. 25331
Thoning, K. W., Tans, P. P., and Komhyr, W. D.: Atmospheric carbon dioxide at Mauna Loa Observatory. II – Analysis of the NOAA GMCC data, 1974–1985, J. Geophys. Res., 94, 8549–8565, doi:10.1029/JD094iD06p08549, 1989. 25333, 25334, 25339, 25347
Tukey, J. W.: Nonlinear (nonsuperposable) methods for smoothing data, in: Conference Record: IEEE EASCON, p. 673, 1974. 25338
Turnipseed, A. A., Anderson, D. E., Burns, S., Blanken, P. D., and Monson, R. K.: Airflows and turbulent flux measurements in mountainous terrain: Part 2: Mesoscale effects, Agr. Forest Meteorol., 125, 187–205, doi:10.1016/j.agrformet.2004.04.007, 2004. 25331, 25333
de Wekker, S. F. J., Ameen, A., Song, G., Stephens, B. B., Hallar, A. G., and McCubbin, I. B.: A preliminary investigation of boundary layer effects on daytime atmospheric $CO_2$ concen-





ACPD
11, 25327–25369, 2011



trations at a mountaintop location in the Rocky Mountains, Acta Geophys., 57, 904–922, doi:10.2478/s11600-009-0033-6, 2009. 25330, 25333

Williams, I. N., Riley, W. J., Torn, M. S., Berry, J. A., and Biraud, S. C.: Using boundary layer equilibrium to reduce uncertainties in transport models and $CO_2$ flux inversions, Atmos. Chem. Phys. Discuss., 11, 11455–11495, doi:10.5194/acpd-11-11455-2011, 2011. 25349

Yi, C., Anderson, D. E., Turnipseed, A. A., Burns, S. P., Sparks, J. P., Stannard, D. I., and Monson, R. K.: The contribution of advective fluxes to net ecosystem exchange in a high-elevation, subalpine forest, Ecol. Appl., 18, 1379–1390, doi:10.1890/06-0908.1, 2008. 25329, 25330

Zupanski, D., Denning, A. S., Uliasz, M., Zupanski, M., Schuh, A. E., Rayner, P. J., Peters, W., and Corbin, K. D.: Carbon flux bias estimation employing Maximum Likelihood Ensemble Filter (MLEF), J. Geophys. Res., 112, D17107, doi:10.1029/2006JD008371, 2007. 25332





ACPD

11, 25327–25369, 2011



**Table 1.** Site details. Listed are the site coordinates, elevations in m a.s.l., inlet height, and installation year. All sites are topographically situated on mountaintops except FEF (alpine valley), and NWR (ridgetop). As discussed previously, measurements from FEF are only used in a specific diagnostic test and are otherwise not used.

| Site | Latitude, Longitude | Elev. (m a.s.l.) | Inlet Hts. (m) | Years |
|---|---|---|---|---|
| FEF | 39.91° N, 105.88° W | 2745 | 2.6,9.5,17.8 | 2005–present |
| RBA | 36.46° N, 109.10° W | 2982 | 3.6,14.3,21.9 | 2007–present |
| SPL | 40.45° N, 106.73° W | 3210 | 2.5,5.8,9.1 | 2005–present |
| HDP | 40.56° N, 111.65° W | 3351 | 17.1,17.8 | 2006–present |
| NWR | 40.05° N, 105.58° W | 3523 | 1.3,3.5,5.1 | 2005–present |





ACPD
11, 25327–25369, 2011



**Table 2.** Filter statistics for the complete set (CS) and each subset (SV, SVLG, SVLR, WM, SI) representing four RACCOON sites HDP, NWR, RBA and SPL (asterisk indicates SVLR statistics exclude HDP data). The retained fraction is computed as the proportion of observations remaining after filtering. Subset means represent the average subset value, and deseasonalized variability indicates the average variability for each subset after removing the seasonal cycle. The topmost sub-table compares subsets when no time-of-day filtering is used, while the lower two sub-tables compare filtering methods when used in combination with time-of-day filtering. Nocturnal filtering targeting downward descending free tropospheric air during hours 00:00, 01:00, 02:00, 03:00 LT (the half-open interval 00:00–04:00 LT) differs from "All Hours" by about +0.3 ppm and from afternoon filtering (12:00–16:00 LT) by about +0.7 ppm.

| Filter | Retained Fraction | Sbst. Mean (ppm) | Deseas. Var. (ppm) |
|---|---|---|---|
| | All Hours | | |
| CS | 1.00 | 387.2 | 5.7 |
| SV | 0.94 | 387.1 | 4.9 |
| SVLG | 0.89 | 387.1 | 4.8 |
| SVLR* | 0.90 | 387.1 | 11.0 |
| WM | 0.45 | 387.0 | 3.7 |
| SI | 0.43 | 387.4 | 9.0 |
| | 00:00-04:00 LT | | |
| CS | 0.17 | 387.5 | 5.5 |
| SV | 0.16 | 387.3 | 4.8 |
| SVLG | 0.15 | 387.4 | 4.7 |
| SVLR* | 0.15 | 387.5 | 4.4 |
| WM | 0.07 | 386.9 | 3.8 |
| SI | 0.10 | 387.3 | 9.3 |
| | 12:00–16:00 LT | | |
| CS | 0.17 | 386.8 | 5.7 |
| SV | 0.15 | 386.8 | 4.9 |
| SVLG | 0.15 | 386.9 | 4.9 |
| SVLR* | 0.14 | 386.6 | 4.7 |
| WM | 0.08 | 387.0 | 3.7 |
| SI | 0.03 | 388.0 | 7.4 |





ACPD
11, 25327–25369, 2011



**Table 3.** The strength of seasonal cycle of $CO_2$ mixing ratios is listed by the difference between seasonal means representing the annual maximum (February, March, April) and minimum (August, September, October) values in ppm $CO_2$ (asterisk indicates SVLR statistics exclude HDP data).

| Filter | Seasonal Diff. | Sum. Mean | Win. Mean |
|---|---|---|---|
| CS | 7.0 | 383.0 | 390.0 |
| SV | 7.0 | 382.8 | 389.8 |
| SVLG | 6.9 | 382.8 | 389.7 |
| SVLR* | 6.7 | 382.9 | 389.6 |
| WM | 6.6 | 382.9 | 389.5 |
| SI | 6.6 | 382.8 | 389.4 |





ACPD
11, 25327–25369, 2011



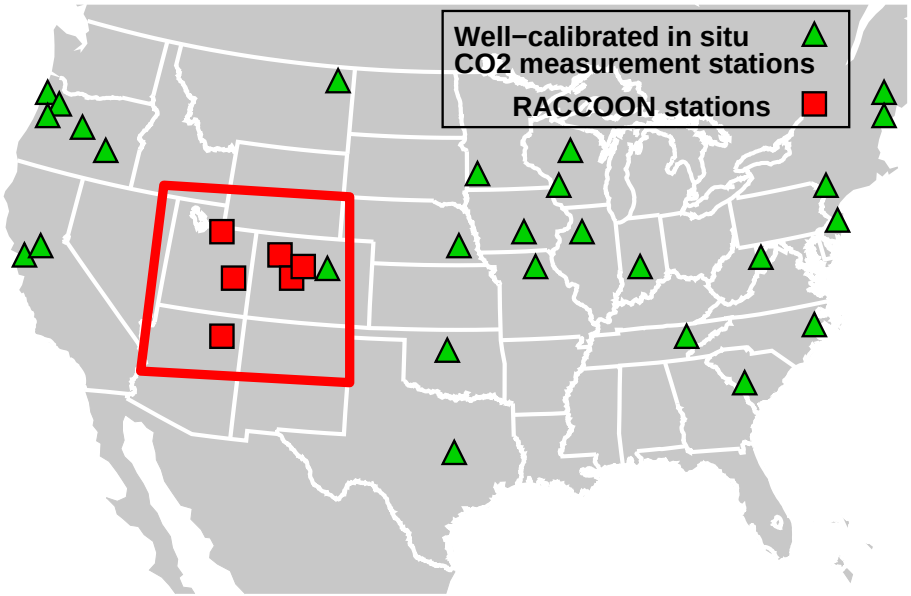


**Fig. 1.** Map of RACCOON domain. The complimentary positioning of the RACCOON mountaintop network of autonomous $CO_2$ mixing ratio surface sites is shown with reference to NOAA's $CO_2$ mixing ratio measurement network, Penn State's Midcontinental Ring 2 sites, the ORCA network, and other well-calibrated in situ $CO_2$ mixing ratio sites in the Continental US.





ACPD
11, 25327–25369, 2011



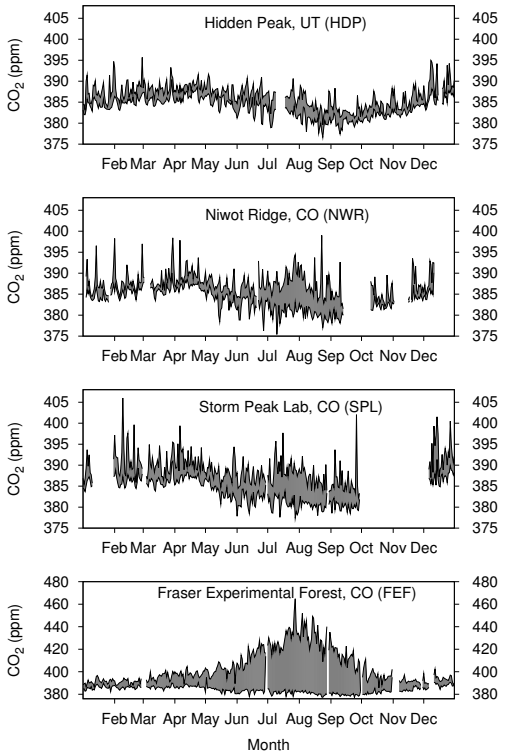


**Fig. 2.** $CO_2$ mixing ratios measured by 4 RACCOON sites for the year 2007. These differences in diurnal and seasonal variability are shown by the area between daily min and max $CO_2$ mixing ratios. Strong positive $CO_2$ spikes are present during winter, and both positive and negative spikes occur during summer. The bottom panel shows mixing ratios from the Fraser Experimental Forest site (see Table 1), which although not intended to make measurements of well mixed mountaintop air, we include in one test in order to distinguish filters using an extreme case from a site that is not ideally situated.





ACPD
11, 25327–25369, 2011



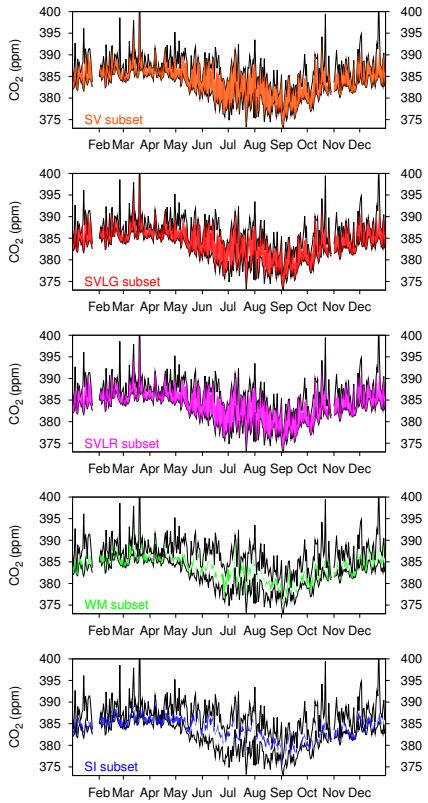


**Fig. 3.** Diurnal and seasonal variability in $CO_2$ mixing ratios from all five filters are contrasted against the complete set of observations using one year of data (2006) from one RACCOON site (Storm Peak, Colorado). This figure shows that hourly statistical filters (SV, SVLG, SVLR) retain a majority of the diurnal variability in $CO_2$, while windowing-filters produce subsets with fewer observations constrained to narrower diurnal ranges.





ACPD
11, 25327–25369, 2011



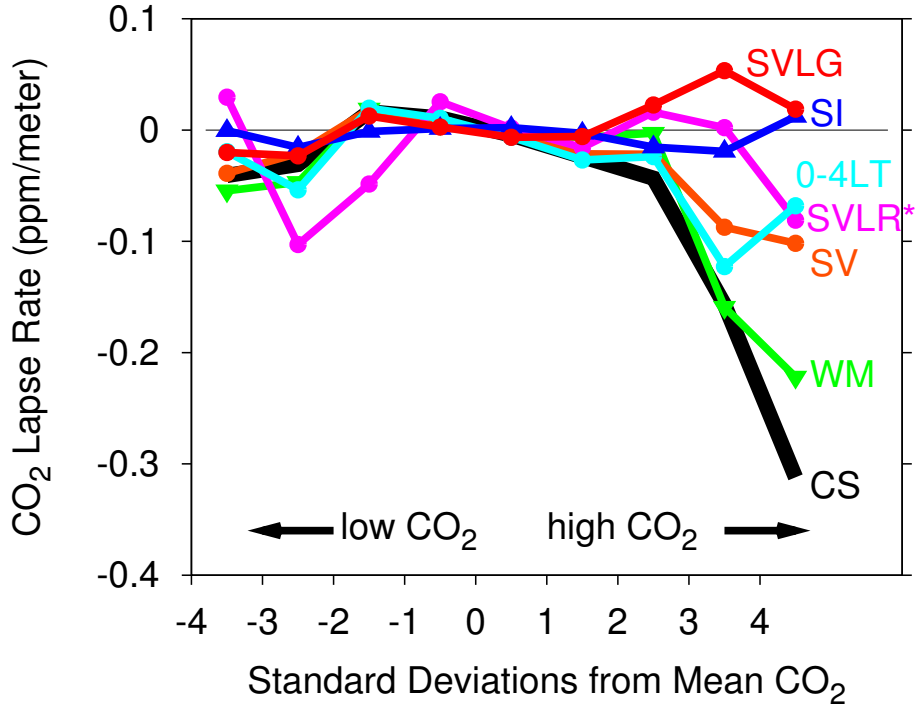


**Fig. 4.** $CO_2$ lapse rates binned by standard deviations from the deseasonalized subset mean. These show the average degree of $CO_2$ stratification in the vicinity of the measurement stations. On the vertical axis ($CO_2$ lapse rate) measurements representing well-mixed conditions appear near-zero, while measurements representing strongly stable conditions have large negative values. On the horizontal axis (standard deviations) measurements typical of afternoon $CO_2$ uptake appear to the left, while nocturnal measurements (tending to have larger $CO_2$ values) appear to the right.





ACPD
11, 25327–25369, 2011



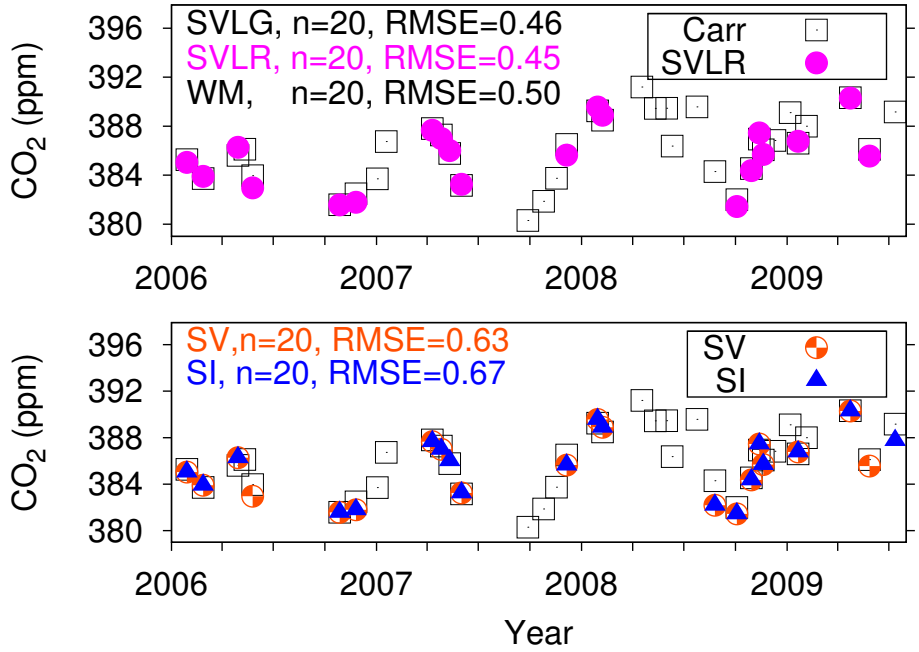


**Fig. 5.** 20 cases of well-mixed air determined from NOAA airborne flights above Carr, Colorado are compared against the corresponding hourly mean measurements from the Niwot Ridge RACCOON site for each filtered subset. Subsets are standardized to equal numbers of measurements. The top panel shows (using SVLR) that SVLG, SVLR and WM subsets have roughly similar error from Carr measurements (RMSE $\approx$ 0.5 ppm) from well-mixed cases at Carr. SI and WM subsets show slightly larger bias (RMSE $\approx$ 0.7 ppm) over the same 20 cases. This suggests that when standardized to a common sample size filters are roughly similar in filtering observations representing well-mixed air, and that this does not resolve how stringent the filter criteria should be.





ACPD
11, 25327–25369, 2011



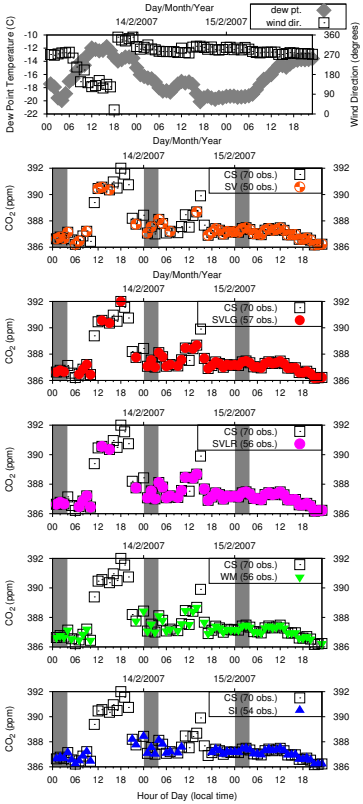


**Fig. 6.** A synoptic case study from NWR site (13–15 February 2007) comparing filtered subsets standardized to retain two-thirds of NWR measurements. The upper plot of meteorology data has dual vertical axes that are listed on the left and right. The number of observations comprising each case study subset is listed in the legend box. The gray band locates the 00:00–04:00 LT interval, which is used by some inversion model systems in place of statistical filtering prior to assimilation.





ACPD
11, 25327–25369, 2011



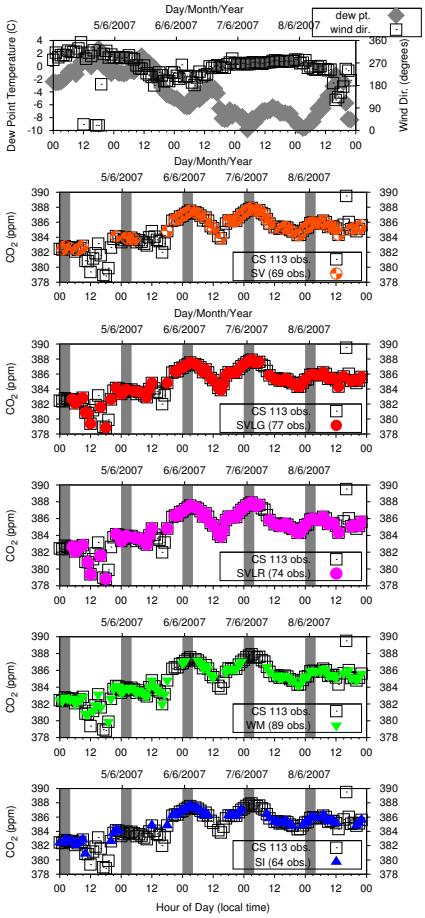


**Fig. 7.** Synoptic case (4–8 June 2007) same as Fig. 6 but with transient wind direction shift near 12:00 LT on 4 June. The gray bands locate 00:00–04:00 LT measurements, which are the hours assimilated by some inversion model systems.





ACPD
11, 25327–25369, 2011



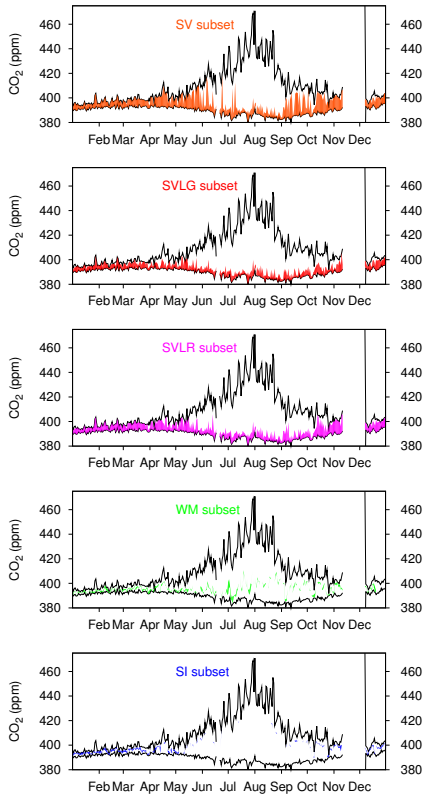


**Fig. 8.** Extracting useful observations from a "difficult-to-model" mountaintop location using one year (2010) of observations from the FEF site, which is strongly influenced by local (within-valley) circulations and strong summertime respiration. This figure reveals an important limitation of windowing-filters, which are not able to identify a realistic seasonal $CO_2$ cycles when diurnal variability is high. This is because SI and WM filters rely on daily mean/median values (or trends) to subset observations. This suggests that windowing-filters (WM, SI) by themselves may not be suitable for continental $CO_2$ measurements.





ACPD
11, 25327–25369, 2011



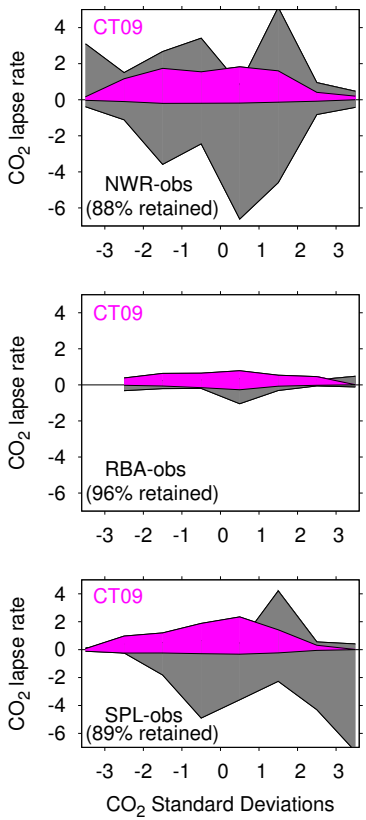


**Fig. 9.** SVLR: Modeled (CT-2009) vs. observed $CO_2$ lapse rates as a function of deseasonalized $CO_2$ lapse rate. The SVLR filter uses $CO_2$ lapse rates limits (colored in magenta) specified by the model atmosphere to constrain $CO_2$ mixing ratios measured at RACCOON sites where the measured $CO_2$ lapse rate is larger than the model can represent (colored gray). Lapse rate limits are time of day and location (HDP, NWR, RBA, SPL) specific.





ACPD
11, 25327–25369, 2011



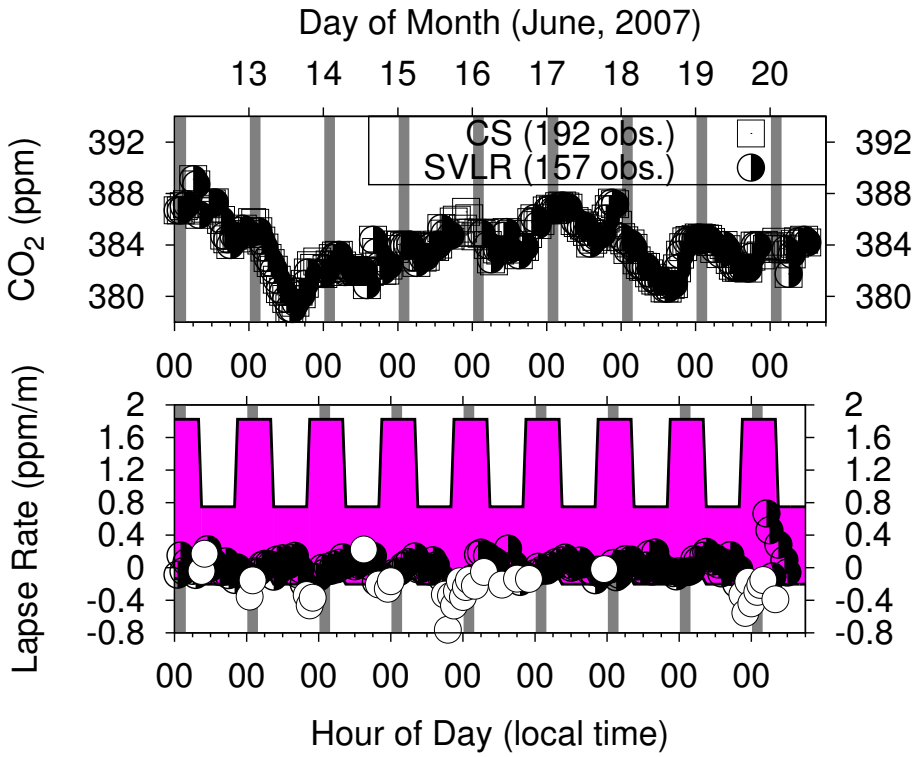


**Fig. 10.** Lapse rate filter case study (12–20 June 2007 at Niwot Ridge). SVLR works by first identifying the range of model $CO_2$ lapse rates (indicated by the diurnally varying magenta band in the lower panel). In the lower panel open circles represent observations with either excessive hourly variance or that fall outside model lapse rate ranges. The upper panel shows the corresponding $CO_2$ mixing ratios.





ACPD
11, 25327–25369, 2011